J. theor. Biol. (2001) **209,** 383–394
doi:10.1006/jtbi.2001.2252, available online at http://www.idealibrary.com on IDEAL®

Modeling of Branching Structures of Plants

WANG ZHI*†, ZHAO MING‡ AND YU QI-XING*

**College of Life Sciences, Wuhan University, Wuhan, Hubei* 430072, *People's Republic of China and*
‡*Automation Department of Tsinghua University, Beijing* 100084, *People's Republic of China*

(*Received on* 25 *August* 1999, *Accepted in revised form on* 4 *December* 2000)

Previous studies of branching structures generally focused on arteries. Four cost models minimizing total surface area, total volume, total drag and total power losses at a junction point have been proposed to study branching structures. In this paper, we highlight the branching structures of plants and examine which model fits data of branching structures of plants the best. Though the effect of light (e.g. phototropism) and other possible factors are not included in these cost models, a simple cost model with physiological significance, needs to be verified before further research on modeling of branching structures is conducted. Therefore, data are analysed in this paper to determine the best cost model. Branching structures of plants are studied by measuring branching angles and diameters of 234 junctions from four species of plants. The sample includes small junctions, large junctions, two- and three-dimensional junctions, junctions with three branches joining at a point and those with four branches joining at a point. First, junction exponents (x) were determined. Second, log–log plots indicate that model of volume minimization fits data better than other models. Third, one-sided t-tests were used to compare the fitness of four models. It is found that model of volume minimization fits data better than other cost models.

© 2001 Academic Press

1. Introduction

It is a popular notion that plants occurring in nature have evolved branching structures which perform their tasks in some optimal way. Branch diameter is one important parameter of branching structures which is closely related to other parameters. Da Vinci (1970) suggested that the cross-sectional area of the parent branch is equal to the sum of the cross-sectional areas of its daughter branches. Barker *et al.* (1973) related diameter to order of branching in apple and birch trees giving linear plots when the logarithm of diameter is plotted against order. He also indicated that the number of buds or branches is proportional to diameter. In 1955, Jessen found that the number of fruits distal to a given point is a function of the cross-sectional area of the branch at that point (quoted by Barker *et al.*, 1973). Murray (1927) showed that the weight of a branch distal to a given point is a power function of the circumference at that point. McMahon & Kronauer (1976) demonstrated the existence of a high positive correlation coefficient between diameters and lengths from random twigs to the trunk in a large white oak. All these conclusions are extensions of the *pipe model* proposed by Shinozaki *et al.* (1964). This model regarded a branch as a pipe. Each unit pipe supports a "unit amount of photosynthetic organs", e.g. a constant number of leaves. Each pipe connects a leaf to the tree's trunk, i.e. the

† Author to whom correspondence should be addressed.
E-mail: wzhizooo@amexol.net

0022–5193/01/080383 + 12 $35.00/0
© 2001 Academic Press

pipe starts at a corresponding leaf and goes down the entire length of the tree to the base of its trunk. Thus, a trunk can be seen as bundles of pipes connecting leaves. It is plausible that the diameter of a parent branch should have a relationship with that of a daughter branch.

Occurring often in nature, branching structures of arteries and rivers have been studied in detail by many investigators (Murray, 1926a, b; Leopold, 1971; Zamir *et al.*, 1983; Zamir & Bigelow, 1984; Roy & Woldenberg, 1982; Woldenberg & Horsfield, 1983, 1986; and others cited in these works). The essence of their research is to compare the fitness of four models minimizing a parameter called "cost". These four costs are surface area, volume, drag (shear stress) and power losses. Model of surface minimization and model of volume minimization are "flow-independent" because these cost functions depend on only diameter, not flow rates. Model of drag minimization and model of power minimization are "flow-dependent" because these cost functions depend on both vessel diameter and flow rate.

Actually, there are many factors affecting the branching structures of plants. Light, gravity and other environmental factors may have an influence on the branching structures. A hypothesis is proposed that cost minimization also happens in the branching structures of plants.

This paper is an attempt to find the best one among these four cost models of fitting data of branching structures of plants. Such verification will help us to examine whether cost minimization happens in plants in the future. Our investigation is also motivated by potential practical applications such as computer simulation of plant shape and so on.

Murray (1927) indicated that model of volume minimization might be applied to botanical trees. We furthered his research and found that model of volume minimization is really better than other models in fitting data of branching structures of plant. As far as we know, data of branching angles and diameters are not available in adequate quantity. We filled in this gap. In this paper, data of two- and three-dimensional branching structure of four species of plants are presented.

This paper is organized as follows. In Section 2, we introduce all definitions, theoretical equations and four models of cost minimization. In Section 3, the method of measuring branching structures of plants is described. Junction exponents are calculated. Data of measurements are plotted on log–log plots. The *t*-tests are conducted to compare the error of each model. In Section 4, plots and statistics of *t*-tests are analysed. In Section 5, sources of error and variation are discussed.

2. Theoretical Consideration

It is assumed that branches are perfect (non-tapering) cylinders in this paper. Figure 1(a) illustrates a typical two-dimensional junction with three branches. The "cost" per unit length (C) may be surface area, volume, drag (shear stress) and power losses depending on the model considered. Assuming that $A(x_2, y_2)$, $B(x_3, y_3)$, $C(x_1, y_1)$ and $M(x, y)$, respectively, represent coordinates of two ending points of daughter branches, the starting point of the parent branch, and the junction point, $f(x, y)$ shown by eqn (1) is the total cost of the junction from C to A and B.

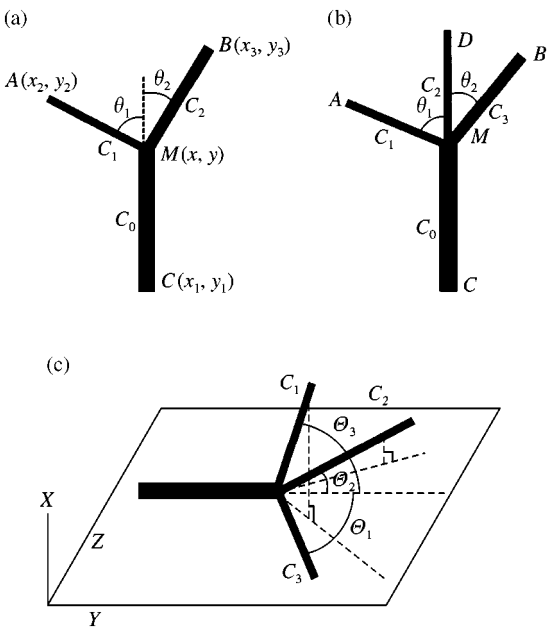

FIG. 1. C_0, C_1, C_2 and C_3 refer to the cost per unit length of parent branch and daughter branches. θ_1, θ_2 and θ_3 are branching angles. ψ is junction angle. (a) Three branches at a junction. (b) Four branches at a two-dimensional junction. θ_3 is the branching angle between daughter branch MD and parent branch CM. $\theta_3 = 0$. (c) Four branches at a three-dimensional junction $\theta_3 \neq 0$.

Subscripts 0, 1, and 2 refer to the parent, major and minor daughter branches. The major and minor branching angles are θ_1 and $\theta_2(\theta_1 > \theta_2)$. The junction angle ψ is $\theta_1 + \theta_2$. The radicals represent the respective lengths of each branch:

$$f(x, y) = C_0\sqrt{(x - x_1)^2 + (y - y_1)^2} + C_1\sqrt{(x - x_2)^2 + (y - y_2)^2} + C_2\sqrt{(x - x_3)^2 + (y - y_3)^2}. \quad (1)$$

The minimum of total cost $f(x, y)$ can be achieved when x and y have certain values. To explain in geometric terms, minimization may be achieved by moving the junction point in the X and Y directions. By setting the derivatives with respect to x and y to zero, eqns (2) and (3) are obtained. Equation (2) is the condition for minimization with Y, which represents a relationship between parent branch and daughter branches. Equation (3) is the condition for minimization with X, which represents a relationship between two daughter branches. Equation (3) can be used to explain a common observation proposed by Da Vinci (1970) that for two sibling branch segments the larger sibling deviates less from the parent branch than its smaller sibling:

$$C_1 \cos\theta_1 + C_2 \cos\theta_2 = C_0, \quad (2)$$

$$C_1 \sin\theta_1 = C_2 \sin\theta_2. \quad (3)$$

For a two-dimensional junction with four branches [Fig. 1(b)], the equations can be obtained in the same way. By taking derivatives, the condition for minimization with Y is changed to eqn (4). The condition for minimization with X is still eqn (3):

$$C_1 \cos\theta_1 + C_2 \cos\theta_2 + C_3 = C_0. \quad (4)$$

For a three-dimensional junction with four branches [Fig. 1(c)], the equations can also be obtained in the same way. Suppose the direction of the parent branch is Y direction and an XZ plane is perpendicular to the parent branch, by taking derivatives the condition for minimization with Y is eqn (5). Given the complexity of angle, it is hard to examine the condition of minimization with X and the condition of minimization with Y. We have not studied two potential equations similar to eqn (3):

$$C_1 \cos\theta_1 + C_2 \cos\theta_2 + C_3 \cos\theta_3 = C_0. \quad (5)$$

A real plant usually has three types of branching structures—alternate, opposite and whorled. Junctions with three branches originate from the alternate pattern. Junctions with four branches originate from the opposite pattern. Junctions with more than four branches originate from the whorled pattern. Therefore, in measurement two other patterns of junctions were considered [Fig. 1(b) and (c)]. One pattern is a two-dimensional junction with four branches, the other is a three-dimensional one with four branches. Subscript 3 refers to the third daughter branch; θ_3 is its branching angle.

Zamir (1976) has summarized four models of cost minimization which have been proposed to explain branching angles in arteries. These four models—minimum surface, volume, drag and power—fall into two categories. Model of surface minimization and model of volume minimization are "flow-independent". Minimum surface probably implies a minimum volume of the tissue of the vessel; the minimum volume criterion minimizes the volume of the fluid. Model of drag minimization and model of power minimization are "flow-dependent". The drag criterion minimizes the drag on the walls of the vessel and the power criterion minimizes the power losses incurred in moving the fluid. For branching structures of plants the applications of these models are not the same. Minimum surface implies a minimum volume of the bark; the minimum volume criterion minimizes the volume of the tissue of the branchwood. Since the inner part of a plant branch is not vacant and is filled with tissues, the application of the two "flow-dependent" models to plant junctions is questionable. Barker *et al.* (1973) stated "although flow doesn't occur in the same way as it does in tubular structures, the transport of sap in a branch may nevertheless be a function of diameter". Therefore, it is necessary to test the fitness of both the two "flow-dependent" models and the two "flow-independent" models.

TABLE 1
Cost factors

Models	Total cost/length (with constants)*	Branch cost
Surface	$(2\pi)r$	r
Volume	$(\pi)r^2$	r^2
Drag	$(8\eta)Qr^{-2} = (8\eta k^x)r^{x-2}$	r^{x-2}
Power	$(8\eta)Q^2r^{-4} = (8\eta k^{2x})r^{2x-4}$	r^{2x-4}

*η is the dynamic viscosity of the fluid and Q is the flow. k and x are constants in the equation $Q = kr^x$.

The flow can be estimated with the following (Murray, 1926a):

$$Q = kr^x, \tag{6}$$

where Q is the flow, k is a constant, r is the radius of an individual branch, and x is a positive exponent defined as junction exponent. If the sinks of water and minerals in the branch itself are not considered, eqn (7) exists for a junction containing n branches, where i denotes individual branches and Q_0 is the total flow in the junction.

Let r_0 be the radius of the parent branch, then from eqns (6) and (7), we get eqn (8).

The value of x at a junction can be determined by iteration only when r_0 is larger than every r_i or smaller than every r_i.

The cost factors for the four models are presented in Table 1 (Woldenberg & Horsfield, 1983, 1986).

$$Q_0 = \sum_{i=1}^{n} Q_1, \tag{7}$$

$$1 = \sum_{i=1}^{n} \left(\frac{r_i}{r_0}\right)^x. \tag{8}$$

When cost factors are inserted into eqns (2) and (3), we have
Minimum surface:

$$r_1 \cos\theta_1 + r_2 \cos\theta_2 = r_0, \tag{9}$$

$$r_1 \sin\theta_1 = r_2 \sin\theta_2. \tag{10}$$

Minimum volume:

$$r_1^2 \cos\theta_1 + r_2^2 \cos\theta_2 = r_0^2, \tag{11}$$

$$r_1^2 \sin\theta_1 = r_2^2 \sin\theta_2. \tag{12}$$

Minimum drag:

$$r_1^{x-2} \cos\theta_1 + r_2^{x-2} \cos\theta_2 = r_0^{x-2}, \tag{13}$$

$$r_1^{x-2} \sin\theta_1 = r_2^{x-2} \sin\theta_2. \tag{14}$$

Minimum power:

$$r_1^{2x-4} \cos\theta_1 + r_2^{2x-4} \cos\theta_2 = r_0^{2x-4}, \tag{15}$$

$$r_1^{2x-4} \sin\theta_1 = r_2^{2x-4} \sin\theta_2. \tag{16}$$

The following parameters are defined for the cases of three branches at a junction. In order to study the fitness of eqns (9), (11), (13) and (15) we should define some parameters to show the error of each equation and do t-tests. According to eqn (2), the theory predicts that $C_1 \cos\theta_1 + C_2 \cos\theta_2$ equals C_0. Hence, the theoretical ratio of the left-hand side (l.h.s.) items and the right-hand side (r.h.s.) items is 1. However, in our measurements this is not the case. Therefore, we defined the following parameters to facilitate the statistical analysis. R_1 is defined as the ratio of the l.h.s. items (e.g. $C_1 \cos\theta_1 + C_2 \cos\theta_2$) and the r.h.s. items (e.g. C_0) of eqn (2). Since R_1 is probably not equal to 1, E_1 is defined as the error of eqn (2)—the absolute value of the difference between 1 and R_1. Likewise, in order to test the fitness of eqns (10), (12), (14) and (16), R_2 is defined as the ratio of the l.h.s. items and the r.h.s. items of eqn (3). Since the l.h.s. and the r.h.s. items of eqn (3) can interchange, the ratio is calculated by dividing the larger one by a smaller one. When R_2 is not less than 1, E_1 is defined as the error of eqn (3)—the value of R_2 minus 1. They are defined by eqns (17)–(20).

In our study, t-tests are used to find out the best one of these four models by comparing the mean of E_1 and E_2 among the four models. ME_1 is defined as the mean of the individual error E_1 of eqn (2). ME_2 is the mean of the individual error E_2 of eqn (3). It is easy to use one-sided t-tests to compare these four ME_1 and four ME_2. The best model must be the one whose ME_1 and ME_2 are the least. ME_1 and ME_2 are given by the following equations (n is sample size, i denotes an individual junction):

Only the equation for calculating the error of three branches at a junction is listed here. For the

cases of four branches at a junction, similar equations including a C_3 item are used to calculate R_1, R_2, E_1, E_2, ME_1 and ME_2. For simplicity, they are omitted here. But they are used to calculate the statistics:

$$R_1 = \frac{C_1 \cos\theta_1 + C_2 \cos\theta_2}{C_0}, \tag{17}$$

$$E_1 = |R_1 - 1|, \tag{18}$$

$$R_2 = \frac{\max\{C_1 \sin\theta_1, C_2 \sin\theta_2\}}{\min\{C_1 \sin\theta_1, C_2 \sin\theta_2\}}, \tag{19}$$

$$E_2 = |R_2 - 1| = R_2 - 1, \tag{20}$$

$$ME_1 = \frac{\sum_{i=1}^{n} E_{1i}}{n}, \tag{21}$$

$$ME_2 = \frac{\sum_{i=1}^{n} E_{2i}}{n}. \tag{22}$$

3. Results

The measurements were taken from four species of plants including two shrubs—Chinese Redbud and Sweet Osmanthus, one form of Hairyleaf Japanese Cherry—*Prunus serrulata* Lindl. *f. roseo.* and Southern Magnolia. They are easy to find in Wuhan University (Wuhan, P. R. China). The size of each junction from the two shrubs is small, whose diameters of the parent branches range from 10.8 to 1.8 mm. The size of each junction from Hairyleaf Japanese Cherry is large, whose diameters of the parent branches range from 172 to 24 mm. In previous research of branching structures of plants, data of junctions with four branches joining at a point and three-dimensional junctions are not reported. They are included in the samples in this paper.

Two hundred and thirty four junctions were measured, 50 from Chinese Redbud, 104 from Sweet Osmanthus, 50 from Hairyleaf Japanese Cherry and 30 from Southern Magnolia. All junctions from Chinese Redbud, 50 junctions of Sweet Osmanthus and all junctions from Hairyleaf Japanese Cherry each have three branches joining at a point [Fig. 1(a)]. Fifty four junctions from Sweet Osmanthus each have four branches [Fig. 1(b)] with the middle daughter branch lying along the pathway of parent branch. Thirty three-dimensional junctions from Southern Magnolia each have four branches [Fig. 1(c)]. These five samples are identified in Table 2.

Data of Zamir *et al.* (1983) demonstrated that in arteries branches of a junction have a strong tendency to lie in a plane. The same case is with three branches joining at a point in plant according to our observations. Among 150 junctions with three branches from Chinese Redbud, Sweet Osmanthus and Hairyleaf Japanese Cherry, nearly all the branches joining at a junction lie in a plane and most of them are straight. Probably, there are some other unknown principles that cause their junction branches to lie in a

TABLE 2
Identification of the specimens whose junctions are studied

Species	Common name	Type of junctions	No.	d_0 (mm)	X	ψ
Cercis chinensis	Chinese Redbud	Three branches at a junction (two-dimensional)	50	5.21 (2.28–9.05)	3.41 (2.30–4.90)	61.34 (32–89)
Osmanthus fragrans	Sweet Osmanthus	Three branches at a junction (two-dimensional)	47	5.08 (3.53–7.00)	2.57 (0.85–4.65)	58.14 (34–77)
Prunus serrulata Lindl. *f. roseo.*	One form of Hairyleaf Japanese Cherry	Three branches at a junction (two-dimensional)	47	85.04 (24.51–172.5)	2.12 (1.62–4.19)	46.85 (19–86)
Osmanthus fragrans	Sweet Osmanthus	Four branches at a junction (two-dimensional)	51	6.17 (3.40–10.80)	3.11 (1.90–6.56)	— —
Magnolia grandiflora	Southern Magnolia	Four branches at a junction (three-dimensional)	30	14.58 (8.68–28.08)	3.05 (1.88–4.90)	— —

Note: d_0 = mean and range of diameter (mm) of the parent branch; X = mean and range of the junction exponents x; ψ = mean and range of the observed junction angle ($\theta_1 + \theta_2$); — = data are not available.

plane. They need to be determined in the future. But it is not related to our study now. We merely regard the phenomena as an assumption of our model. Therefore, for junctions with three branches all measurements were derived from two-dimensional branching structures. It is also observed that nearly all branch segments in our measurements are cylinders. So it is valid to apply these four models.

Measurement of diameter (d) and branching angle (θ) is illustrated in Fig. 2. Each segment of a branch is between two points of junction, or between a junction and the first bud. For a small junction, diameter was measured twice by caliper with a vernier scale to the nearest 0.1 mm, across the greatest diameter. One measurement was taken at a point near the junction, the other was taken at a point midway between the junction point and the ending point of the segment or the first bud. Diameter is the average of two measurements. Branching angles θ_1 and θ_2 are measured, too. Where possible, the angle was taken between the tangent of daughter branch starting from the junction point and the axis of parent branch, so avoiding the deflection often found in branch segments.

Junction exponents, x, were found by solving eqn (8) for x with an iterative search routine. Data were processed by a computer program which was able to calculate the junction exponent x for each junction.

Within the 234 junctions, three junctions with three branches and three with four branches from Sweet Osmanthus were unusable while calculating the exponent x since the diameter of the daughter branch is a little larger than that of the parent branch. Measurement error and the irregularity of the branch segment might cause it. In our sample more than 97% junctions are useful for calculating the exponent x. Hence, we do not think that discarding these six junctions will affect testing these four models. In addition, three junctions from Hairyleaf Japanese Cherry are discarded because one branching angle is 0 so that R_2 cannot be calculated. It may also be caused by the measurement error.

Our statistics comes from 225 usable junctions. Average values of x for each type of junctions are listed in Table 2. Data of diameter of the parent branch d_0, the junction angle and the junction exponents are also listed in Table 2. Frequency distribution of junction exponents of 225 junctions is constructed in Fig. 2.

Expected values of C_0 were plotted against the observed C_0 in the double-logarithmic plots, Fig. 3(a), (b), (c) and (d), respectively, representing model of surface, volume, drag and power. For junctions with three branches expected values of C_0 equals $C_1 \cos\theta_1 + C_2 \cos\theta_2$. For two-dimensional junctions with four branches expected values of C_0 are equal to $C_1 \cos\theta_1 + C_2 \cos\theta_2 + C_3$. For three-dimensional junctions with four branches expected values of C_0 are equal to $C_1 \cos\theta_1 + C_2 \cos\theta_2 + C_3 \cos\theta_3$. For each model, the cost factor is chosen according to Table 1. The radius r is half of the diameter d, so calculating the cost factor listed in Table 1 with d instead of r had no impact on the results of testing these four models. The fitness of eqns (2), (4) and (5) can be compared among four models by observing whether these points fall on the solid line $y = x$.

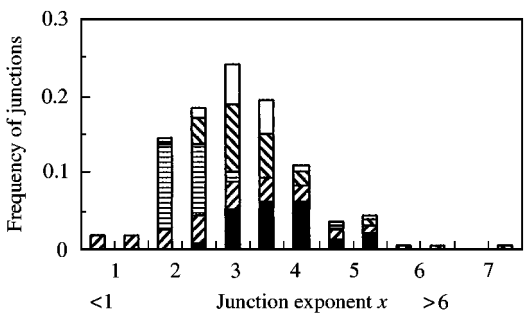

FIG. 2. Vertically stacked frequency distributions of junction exponents of 225 junctions. (□) 30 junctions with four branches from Southern Magnolia; (▨) 51 junctions with four branches from Sweet Osmanthus; (▤) 47 junctions with three branches from Hairyleaf Japanese Cherry; (▨) 47 junctions with three branches from Sweet Osmanthus; (■) 50 junctions with three branches from Chinese Redbud.

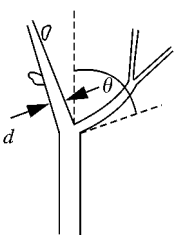

FIG. 3. Measurement of diameter between the junction point and the first bud or the second junction point. Measurement of branching angle between the tangent of a daughter branch and the axis of the parent branch.

$\text{Max}\{C_1 \sin\theta_1, C_2 \sin\theta_2\}$ were plotted against $\min\{C_1 \sin\theta_1, C_2 \sin\theta_2\}$ in the double-logarithmic plots, where data of four models are shown in four plots [Fig. 4(a), (b), (c) and (d)], respectively, representing model of surface area, volume, drag and power. The fitness of eqn (3) can be compared for four models in the same way.

For the 30 three-dimensional junctions from Southern Magnolia, branching angles were measured between the tangent of each daughter branch and the axis of the parent branch [Fig. 1(c)]. The relationship among $C_1 \sin\theta_1$, $C_2 \sin\theta_2$ and $C_3 \sin\theta_3$ is very difficult to determine compared to a two-dimensional junction so that we determined to merely test eqn (5).

For five samples of plant, ME_1 and ME_2 are calculated according to every cost model. Subscripts s, v, d, and p are used to denote the surface model, the volume model, the drag model and the power model. One-sided t-tests are conducted to compare different ME_1 or ME_2 from different models. Student's t-statistics with associated p values are listed in Table 3 according to each one-sided t-test.

Figure 4(a)–(d) shows the data from 225 junctions of these four models. Figure 4(a) shows the

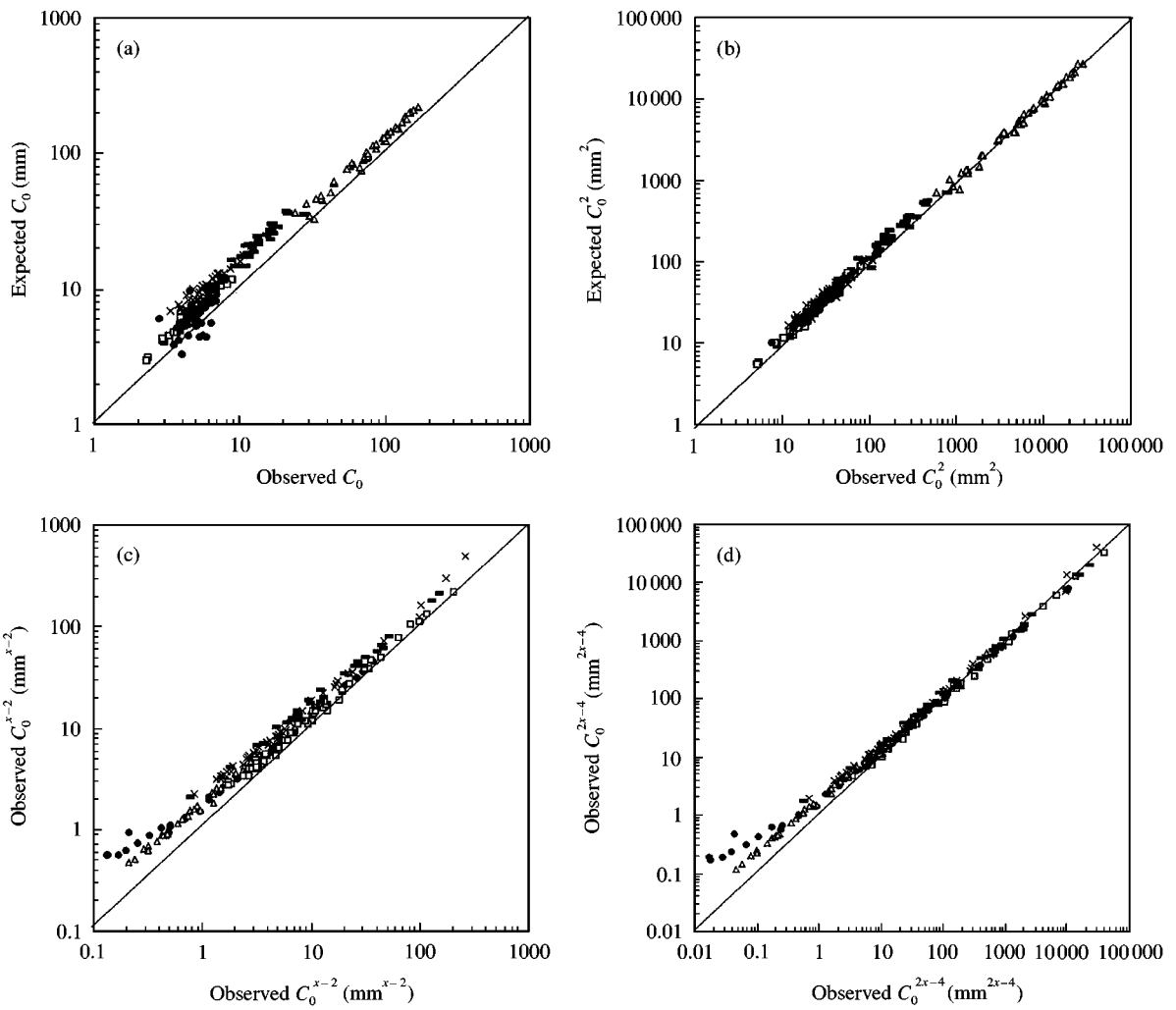

FIG. 4. Expected C_0 vs. C_0 for 225 junctions. The solid line in each plot limits the location of points because all points should locate on the solid line $y = x$ according to the model. (a) Expected C_0 vs. observed C_0. (b) Expected C_0^2 vs. observed C_0^2. (c) Expected C_2^{x-2} vs. observed C_0^{x-2}. (d) Expected C_0^{2x-4} vs. observed C_0^{2x-4}. (□) 50 junctions from Chinese Redbud (three branches at a junction); (●) 47 junctions from Sweet Osmanthus (three branches at a junction); (▲) 47 junctions from Hairyleaf Japanese Cherry (three branches at a junction); (×) 51 junctions from Sweet Osmanthus (four branches at a junction); (▬) 30 junctions from Southern Magnolia (four branches at a junction).

TABLE 3
List of statistics of t-tests

		Minimum surface model (s)	Minimum volume model (v)	Minimum drag model (d)	Minimum power model (p)
Cercis chinensis	ME_1	0.356	0.113	0.277	0.134
(Three branches at	H_0:	$ME_{1s} = ME_{1v}$	$ME_{1v} = 0$	$ME_{1d} = ME_{1v}$	$ME_{1p} = ME_{1v}$
a junction)	H_1:	$ME_{1s} > ME_{1v}$	$ME_{1v} > 0$	$ME_{1d} > ME_{1v}$	$ME_{1p} > ME_{1v}$
	t	34.211	9.405	6.514	1.003
	p	<0.0001	<0.0001	<0.0001	0.160
	ME_2	0.583	0.675	0.648	0.987
	H_0:	$ME_{2s} = ME_{2v}$	$ME_{2v} = 0$	$ME_{2d} = ME_{2v}$	$ME_{2p} = ME_{2v}$
	H_1:	$ME_{2s} < ME_{1v}$	$ME_{2v} > 0$	$ME_{2d} < ME_{1v}$	$ME_{2p} > ME_{1v}$
	t	-2.168	7.564	-0.667	2.868
	p	0.018	<0.0001	0.254	0.003
Osmanthus fragrans	ME_1	0.289	0.118	0.786	1.306
(Three branches at	H_0:	$ME_{1s} = ME_{1v}$	$ME_{1v} = 0$	$ME_{1d} = ME_{1v}$	$ME_{1p} = ME_{1v}$
a junction)	H_1:	$ME_{1s} > ME_{1v}$	$ME_{1v} > 0$	$ME_{1d} > ME_{1v}$	$ME_{1p} > ME_{1v}$
	t	7.89	11.619	5.59	3.35
	p	<0.0001	<0.0001	<0.0001	0.0008
	ME_2	0.794	0.765	0.918	0.97
	H_0:	$ME_{2s} = ME_{2v}$	$ME_{2v} = 0$	$ME_{2d} = ME_{2v}$	$ME_{2p} = ME_{2v}$
	H_1:	$ME_{2s} > ME_{1v}$	$ME_{2v} > 0$	$ME_{2d} > ME_{1v}$	$ME_{2p} > ME_{1v}$
	t	0.579	6.861	1.677	1.778
	p	0.283	<0.0001	0.050	0.041
Prunus serrulata	ME_1	0.266	0.095	0.752	0.751
Lindl. *f. roseo.*	H_0:	$ME_{1s} = ME_{1v}$	$ME_{1v} = 0$	$ME_{1d} = ME_{1v}$	$ME_{1p} = ME_{1v}$
(Three branches at	H_1:	$ME_{1s} > ME_{1v}$	$ME_{1v} > 0$	$ME_{1d} > ME_{1v}$	$ME_{1p} > ME_{1v}$
a junction)	t	8.303	9.066	17.455	12.285
	p	<0.0001	<0.0001	<0.0001	<0.0001
	ME_2	2.044	1.682	2.861	2.728
	H_0:	$ME_{2s} = ME_{2v}$	$ME_{2v} = 0$	$ME_{2d} = ME_{2v}$	$ME_{2p} = ME_{2v}$
	H_1:	$ME_{2s} > ME_{1v}$	$ME_{2v} > 0$	$ME_{2d} > ME_{1v}$	H_1:$ME_{2p} > ME_{1v}$
	t	1.465	3.994	2.443	3.170
	p	0.075	0.0001	0.0009	0.0013
Osmanthus fragrans	ME_1	0.683	0.166	0.773	0.424
Four branches at	H_0:	$ME_{1s} = ME_{1v}$	$ME_{1v} = 0$	$ME_{1d} = ME_{1v}$	$ME_{1p} = ME_{1v}$
a junction	H_1:	$ME_{1s} > ME_{1v}$	$ME_{1v} > 0$	$ME_{1d} > ME_{1v}$	$ME_{1p} > ME_{1v}$
(two-dimensional)	t	37.216	9.543	12.705	4.352
	p	<0.0001	<0.0001	<0.0001	<0.0001
	ME_2	0.218	0.410	0.320	0.734
	H_0:	$ME_{2s} = ME_{2v}$	$ME_{2v} = 0$	$ME_{2d} = ME_{2v}$	$ME_{2p} = ME_{2v}$
	H_1:	$ME_{2s} < ME_{1v}$	$ME_{2v} > 0$	$ME_{2d} < ME_{1v}$	$ME_{2p} > ME_{1v}$
	t	-3.428	8.548	-1.24	1.700
	p	0.0006	<0.0001	0.110	0.048
Magnolia grandiflora	ME_1	0.643	0.173	0.708	0.335
Four branches at	H_0:	$ME_{1s} = ME_{1v}$	$ME_{1v} = 0$	$ME_{1d} = ME_{1v}$	$ME_{1p} = ME_{1v}$
a junction	H_1:	$ME_{1s} > ME_{1v}$	$ME_{2v} > 0$	$ME_{1d} > ME_{1v}$	$ME_{1p} > ME_{1v}$
(three-dimensional)	t	22.524	8.268	7.477	2.155
	p	<0.0001	<0.0001	<0.0001	0.020
	ME_2	—	—	—	—

Note: ME_1 = mean error of expected C_0 (refer to left-handed term in eqns (2), (4) and (5)) and observed C_0; ME_2 = mean error of $C_1 \sin\theta_1$ and $C_2 \sin\theta_2$—data are not available. Subscripts s, v, d, and p represent these four models.

result of testing equation (9) of model of surface minimization. Expected C_0 against observed C_0 are plotted in the log–log plot. Almost all points fall above the solid line.

Figure 4(b) shows the result of testing equation (11) of model of volume minimization. Expected C_0^2 against observed C_0^2 are plotted in the log–log plot. Almost all points fall close to the solid line.

Figure 4(c) shows the result of testing equation (13) of model of drag minimization. Expected C_0^{x-2} against observed C_0^{x-2} are plotted in the log–log plot. All points fall above the solid line.

Figure 4(d) shows the result of testing equation (15) of model of power minimization. Expected C_0^{2x-4} against observed C_0^{2x-4} are plotted in the log–log plot. Some points fall above the solid line, others fall close to the line.

Figure 5(a), (b), (c) and (d)—respectively, shows the data from 195 junctions (30 junctions of Southern Magnolia are excluded) to test eqns (10), (12), (14) and (16) for the four models. Plots indicate that all of the four equations have a large variation.

Figure 5(a) shows the result of testing equation (10) of model of surface minimization. $\text{Max}\{C_1 \sin\theta_1, C_2 \sin\theta_2\}$ are plotted against $\min\{C_1 \sin\theta_1, C_2 \sin\theta_2\}$.

Figure 5(b) shows the result of testing equation (12) of model of volume minimization. $\text{Max}\{C_1^2 \sin\theta_1, C_2^2 \sin\theta_2\}$ are plotted against $\min\{C_1^2 \sin\theta_1, C_2^2 \sin\theta_2\}$.

Figure 5(c) shows the result of testing equation (12) of model of drag minimization.

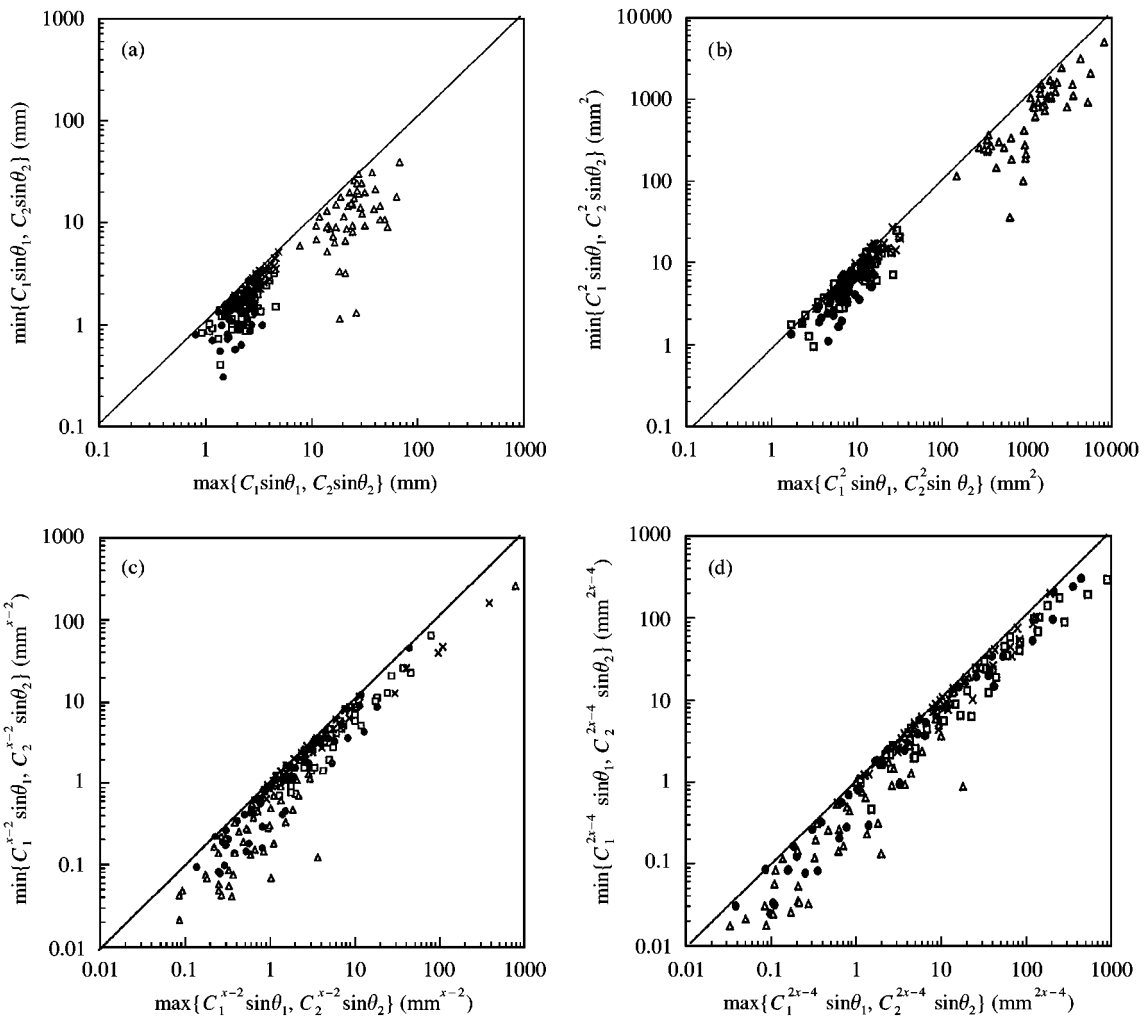

FIG. 5. $\max\{C_1 \sin\theta_1, C_2 \sin\theta_2\}$vs. $\min\{C_1 \sin\theta_1, C_2 \sin\theta_2\}$ for 195 junctions with three branches joining at a point. The solid line in each graph limits the location of points because all points should locate on the solid line $y = x$ according to the model. (a) $\max\{C_1 \sin\theta_1, C_2 \sin\theta_2\}$ vs. $\min\{C_1 \sin\theta_1, C_2 \sin\theta_2\}$. (b) $\max\{C_1^2 \sin\theta_1, C_2^2 \sin\theta_2\}$ vs. $\min\{C_1^2 \sin\theta_1, C_2^2 \sin\theta_2\}$. (c) $\max\{C_1^{x-2} \sin\theta_1, C_2^{x-2} \sin\theta_2\}$ vs. $\min\{C_1^{x-2} \sin\theta_1, C_2^{x-2} \sin\theta_2\}$. (d) $\max\{C_1^{2x-4} \sin\theta_1, C_2^{2x-4} \sin\theta_2\}$ vs. $\min\{C_1^{2x-4} \sin\theta_1, C_2^{2x-4} \sin\theta_2\}$. (□) 50 junctions from Chinese Redbud (three branches at a junction); (●) 47 junctions from Sweet Osmanthus (three branches at a junction); (▲) 47 junctions from Hairyleaf Japanese Cherry (three branches at a junction); (×) 51 junctions from Sweet Osmanthus (four branches at a junction).

$\mathrm{Max}\{C_1^{x-2}\sin\theta_1, C_2^{x-2}\sin\theta_2\}$ are plotted against $\min\{C_1^{x-2}\sin\theta_1, C_2^{x-2}\sin\theta_2\}$.

Figure 5(d) shows the result of testing equation (12) of model of power minimization. $\mathrm{Max}\{C_1^{2x-4}\sin\theta_1, C_2^{2x-4}\sin\theta_2\}$ are plotted against $\min\{C_1^{2x-4}\sin\theta_1, C_2^{2x-4}\sin\theta_2\}$.

Comparing model of surface minimization with model of volume minimization, in all the five samples ME_{1s} is highly significant larger than ME_{1v}. Except that ME_{2s} of junctions with four branches from Sweet Osmanthus is less than ME_{2v}, ME_{2s} of the other three samples are not vastly different from ME_{2v}. Though ME_{2s} of junctions with four branches from Sweet Osmanthus is less than ME_{2v}, ME_{1s} is highly significant larger than ME_{1v}. Hence, we do not think that in this sample model of surface minimization is better than model of volume minimization.

In *t*-tests of comparing model of drag minimization with model of volume minimization, in all five samples ME_{1d} is highly significant larger than ME_{1v}. ME_{2d} of four samples are not less than ME_{2v}.

In *t*-tests of comparing model of power minimization with model of volume minimization, the ME_{1p} of Chinese Redbud has no significant difference from ME_{1v}. In other four samples, the ME_{1p} is highly significant larger than ME_{1v}. ME_{2p} of all five samples are not less than ME_{2v}.

Analysis of *t*-tests suggested that model of volume minimization fit the data better than other models.

4. Discussion

First, it should be mentioned that the global optimum for the total branch volume of a plant is an iterative problem which still remains. It is generally known that as the global optimum is achieved the local optimum of a single junction is often discarded. It will cause variance of cost minimization. The development of branches should be regarded as a dynamic process, i.e. changes of branching angles and branch diameter during growth and shedding of branches according to the circumstances around. McMahon (1976) stated that every tree is continually sensing its own overall geometry, altering its proportions in such a way as to keep that geometry stationary during growth. Honda (1971) stated that ψ (i.e. $\theta_1 + \theta_2$) is concerned with the width or stretch of the whole form of a plant. The value of θ_1 or θ_2 bears a relationship to the degree of "axiality", or deflection of ψ from the main axis of the parent branch. Honda (1971) stated that the interaction among branches; their leaves, seeking sunlight, probably influence the branching greatly. When light interception happens, the growth direction of supporting branch may deflect away from the predetermined direction to obtain more effective leaf surface, with the local optimum destroyed. Phototropism may contribute to make the value of ψ, θ_1 and θ_2 scatter from the optimal values in a local junction, which produces variance.

Second, it is reasonable that power minimization happens in branching structures of plants, since stems have two critical functions of support and transport in vascular land plants. When $x = 3$, the exponent in model of power minimization $2x - 4$ is equal to 2. It is the same as the exponent in model of volume minimization. Hence, as x equals 3, both models will fit the data. Murray (1926a) also showed that simultaneous minimization of viscous power losses and intravascular volume in a segment of artery is achieved when junction exponent $x = 3$. Since much junction, exponents shown in Fig. 2 are close to 3 it is easy to understand that many points are close to $y = x$ in the plot of testing model of power minimization. Junction exponents of large trees are different from that of small trees. It is found that in practice x is about 2.49 for large trees and about 3 for small trees (quoted by Kruszewski & Whitesides, 1998). Our data also agree with such a distinction between small trees and large trees. In our data of x shown in Table 2 and the plot of frequency distribution, the values of x for small junctions are close to 3 and about 2 for large junctions from Hairyleaf Japanese Cherry. It is found that in Fig. 3(d) most points close to the solid line are data from small junctions. Probably, power minimization happens in small junctions rather than in large junctions. The physiological significance of minimization of power losses is obvious, for it would contribute to the "efficiency" of the circulation of sap. The discussion of the reason that power minimization happens in small junction rather than in large junctions is in the following.

Every vascular plant has xylem and phloem to conduct water and nutrients between leaves and roots. Xylem is a conducting tissue made up of cells stacked end to end like the sections of a pipe; these dead cells transport water and minerals. Phloem is a tissue specialized for carbohydrate transport. The cells are stacked vertically end to end to form a tube-like structure. Many pores perforate the end cell walls.

As a non-herbaceous plant matures and grows taller, its stem begins to grow laterally, increasing its diameter. This thickening of the stem, or secondary growth, enables the plant to withstand the added load of branches and leaves, as well as wind, rain, gravity, and other environmental factors. *Biology* (Wessells & Hopson, 1988) stated "as a plant matures, individual cells of both xylem and phloem cease to transport materials; older xylem is often clogged with various substances and no longer transports water and nutrients, phloem elements usually function for only one year or two before dying". New xylem and phloem are produced on the outer side, increasing branch diameter. It is reasonable to assume that as the branch diameter increases the proportion of xylem and phloem to total branch decreases because more dead tissues of them appear in the center. This assumption can be used to explain that model of power minimization that happens in small junctions rather than in large junctions.

Third, it is unlikely to find two identical patterns on living organisms, even though they are presumably genetically homogeneous. Environmental and probabilistic factors should be included in the sources of variation of model of volume minimization. For instance, branches are often curved on account of gravity or sunlight. The gradual change of the direction of branches during growth of the girth (cambial growth) may also increase the measurement error of branching angles. Given that branch segments are not perfect, measurement error of branch diameters will occur.

Fourth, McMahon (1976) stated that there exists a principle of mechanical design—maintenance of elastic similarity. It is possible that branching structures should obey some physical rules limiting the shape of a branch loaded under its weight. Till now we do not know whether the model of volume minimization is the dominant force of designing branching structures. Probably, there are some other principles governing the design including mechanical design and even complex molecular mechanisms. Therefore, even the best cost model—model of volume minimization cannot explain the branching structures of plant very well.

The model represents a theoretical method of determining the branching angles of plants and trees given the diameter of every branch in a junction, which was ever used by (Kruszewski & Whitesides, 1998). The large variance in branching angles is indicated by the large variance in the junction exponents x. The actual branching angle has a considerable scatter from the optimal value. For instance, Fig. 2 shows $x < 2$ in 25 junctions from Hairyleaf Japanese Cherry and 14 junctions with three branches from Sweet Osmanthus. Woldenberg & Horsfield (1986) pointed out that these junctions optimal junction angles cannot be calculated because the values are negative. In eight junctions from Chinese Redbud, one junction from Hairyleaf Japanese Cherry and five junctions with three branches from Sweet Osmanthus $x > 4$, making the optimal junction angles larger than 90°. But actually all observed values of ψ are less than 90°. Even for those x between 2 and 4, a considerable scatter exists between the actual value and the optimal value. These results indicate that a little error of model of volume minimization will result in a large variance of branching angles. Previous workers have noted that experimentally determined branching angles generally exhibit considerable scatter around the theoretical optimum, regardless of which of the four cost models is used for the analysis. However, when actual angles deviate significantly from the predicted optimum, the total "cost" of a junction does not increase by more than a few percent (Zamir *et al.*, 1983; Zamir & Bigelow, 1984).

In conclusion, it is possible to say that model of volume minimization is better than other cost minimization models in fitting data of branching structures of plants. Without including factors such as light and so on, it is not a perfect model to predict the branching structures of plant. Though it does not fit the data very well it provides

us with a new angle to investigate the adaptive functions of branching pattern. The approach of testing the fitness of four models in this paper can be applied to other branching structures such as arteries, neural networks and so on. In addition, this paper will help us to find the principle of designing the branching structures of plants.

This work is partially supported by Professor Guo Youhao, Dr Li Xiangrong, Amy Nail, Zhang Songhua, Liu Fang, Cai Yi, Wang Ying, Dai Jia and Jiang Bo. Especially, we thank Dr Li Xiangrong of Department of Biology in University of Texas A&M for his insightful discussions on modeling. In addition, the referee's valuable suggestions were of much help. Without his hard work, the paper could not have been accomplished.

REFERENCES

BARKER, S. B., CUMMING, G. & HORSFIELD, K. (1973). Quantitative morphometry of the branching structure of trees. *J. theor. Biol.* **40,** 33–43.

DA VINCI, L. (1970). Botany for painters. In: *The Literary Works of Leonardo Da Vinci* (Richter, J. P., ed.), 3rd Edn. New York: Phaidon Publishers Ins.

HONDA, H. (1971). Description of the form of trees by the parameters of the tree like body: effects of the branching angle and the branch length of the shape of the tree like body. *J. theor. Biol.* **31,** 331–338.

KRUSZEWSKI, P. & WHITESIDES, S. (1998). A general random combinatorial model of botanical trees. *J. theor. Biol.* **191,** 221–236.

LEOPOLD, L. B. (1971). Trees and streams: the efficiency of branching patterns. *J. theor. Biol.* **31,** 339–354.

MCMAHON, T. A. & KRONAUER, R. E. (1976). Tree structures: deducing the principle of mechanical design. *J. theor. Biol.* **59,** 443–466.

MURRAY, C. D. (1926a). The physiological principle of minimum work—the vascular system and the cost of blood volume. *Proc. Natl Acad. Sci. U.S.A.* **12,** 207–214.

MURRAY, C. D. (1926b). The physiological principle of minimum work applied to the angle of branching of arteries. *J. General Physiol.* **9,** 835–841.

MURRAY, C. D. (1927). A relationship between circumstance and weight in trees and its bearing on branching angles. *J. General Physiol.* **10,** 725–729.

ROY, A. G. & WOLDENBERG, M. J. (1982). A generalization of the optimal models of arterial branching. *Bull. Math. Biol.* **44,** 349–360.

SHINOZAKI, K., YODA, K., HOZAMI, K. & KIRA, T. (1964). A quantitative analysis of plant form—the pipe model theory—I. Basic analysis. *Jap. J. Ecol.* **14,** 97–105.

WESSELLS, N. K. & HOPSON, J. L. (1988). *Biology*, 1st Edn. New York: Random House.

WOLDENBERG, M. J. & HORSFIELD, K. (1983). Finding the optimal lengths for three branches at a junction. *J. theor. Biol.* **104,** 301–318.

WOLDENBERG, M. J. & HORSFIELD, K. (1986). Relation of branching angles to optimality for four cost principles. *J. theor. Biol.* **122,** 187–204.

ZAMIR, M. (1976). Optimality principles in arterial branching. *J. theor. Biol.* **62,** 227–251.

ZAMIR, M. & BIGELOW, D. C. (1984). Cost of departure from optimality in arterial branching. *J. theor. Biol.* **109,** 401–409.

ZAMIR, M., WRIGLEY, S. M., LANGILLE, B. L. (1983). Arterial bifurcations in the cardiovascular system of a rat. *J. General Physiol.* **81,** 325–335.

APPENDIX A

List of Symbols

$\theta_1, \theta_2, \theta_3$	branching angle
ψ	junction angle, i.e. the sum of $\theta_1 + \theta_2$
C_0	the cost per unit length of parent branch
C_1, C_2, C_3	the cost per unit length of daughter branches
d_0	diameter of parent branch
x	junction exponent
η	the dynamic viscosity of fluid
Q	the flow
r	radius of a branch
R_1	the ratio of the l.h.s. items and the r.h.s. items of eqns (2), (4) and (5)
R_2	the ratio of the l.h.s. items and the r.h.s. items of eqn (3)
E_1	error of expected C_0 and actual C_0
E_2	error of $C_1 \sin\theta_1$ and $C_2 \sin\theta_2$
ME_1	mean error of expected C_0 and actual C_0
ME_2	mean error of $C_1 \sin\theta_1$ and $C_2 \sin\theta_2$
t	Student's t
p	p value